A myriad of other design combinations seem to be available, as simple extrapolations of this proven design, but they have not been seriously considered for likely appearance of other practical problems. By using a CMP-02 type comparator with input offset current specifications of 10 nA/max. and response speed of 250 ns/typical, a many-hundred-channel analog input, 8-bit output magnitude, at a conversion rate of 0.25 MHz, appears possible. Speed of conversion gains much greater than those demonstrated are unlikely, because of the many components the signals must circulate through for each magnitude bit. An estimate would suggest as an example a 16-channel analog input with 4-bit output magnitude resolution at a conversion rate of 2 MHz as an upper limit for this type of circuit.

Acknowledgment

The authors express their gratitude to James Pappin for developing the LABVIEW data acquisition program used in this paper, and for pre-testing it on a conventional A/D converter.

References

[1] S. Soclof, *Applications of Analog Integrated Circuits*. Englewood Cliffs, NJ: Prentice-Hall, 1985.
[2] B. M. Gordon, "Linear electronic analog/digital conversion architectures, their origins, parameters, limitations, and applications," *IEEE Trans. Circuits Syst.*, vol. CAS-25, pp. 391–418, July 1978.
[3] Y. Ichioka and J. Tanida, "Optical parallel logic gates using a shadow-casting system for optical digital computing," *Proc. IEEE*, vol. 72, pp. 787–801, July 1984.
[4] D. Casasant and E. Baranoski, "Directed graph for adaptive organization and learning of a knowledge base," *Applied Optics*, vol. 27, pp. 534–540, 1988.
[5] A Moopenn, J. Lambe, and A. P. Thakoor, "Electronic implementation of associative memory based on neural network models," *IEEE Trans. Syst. Man, Cybern.*, vol. SMC-17, pp. 325–331, Mar./Apr. 1987.
[6] R. A. Athale, H. H. Szu, and C. B. Friedlander, "Optical implementation of associative memory with controlled nonlinearity in the correlation domain," *Opt. Lett.*, vol. 11, pp. 482–484, July 1986.
[7] Labview™, National Instruments Corp., 12109 Technology Boulevard, Austin, TX 78727-6204.

Frequency Domain Analysis of Hopf Bifurcations in Electric Power Networks

H. G. KWATNY AND G. E. PIPER

Abstract—**In this paper we discuss an approach for studying certain types of parametric instabilities in electric power networks that are associated with a Hopf bifurcation. The frequency domain version of the Hopf bifurcation theorem due to Mees and Chua [9] allows us to complete the example of power system flutter instability described by Kwatny and Yu [7].**

I. Introduction

In power systems analysis, stability of an equilibrium point is often determined by investigation of the linearized dynamics. When system parameters vary, so does the linearized model and stability of the equilibrium point may be lost. When this occurs, it typically takes place in either of two ways: a single real eigenvalue of the linearized dynamics or a pair of complex conjugate eigenvalues crosses the imaginary axis. Loss of linear system stability in the former case is sometimes called a "divergence instability" and in the latter a "flutter instability." A complete understanding of the underlying mechanics of the instability can only be obtained, however, by an analysis of the nonlinear system dynamics. In nonlinear dynamics parlance, when the instability is associated with the variation of a single parameter the divergence instability is typically a saddle-node static bifurcation and the flutter instability is typically a Hopf bifurcation.

There has been an erroneous perception that Hopf bifurcations do not occur in power systems. Some of this attitude may be due to comments in Venikov *et al.* [12] that suggest that flutter instabilities are not likely in normal power system operations, and also to some results of Arapostathis *et al.* [3] who argue that the classical swing equations with lossless lines and damping do not possess (so-called type one) periodic solutions. On the other hand, evidence of the occurrence of Hopf bifurcations does exist. In [10], van Ness *et al.* suggest that an observed oscillation is associated with a Hopf bifurcation. Abed and Varaiya [1] illustrate subcritical Hopf bifurcations in a two-machine model with a lossy transmission line. Alexander [2] provides a complete analysis of this case and demonstrates the occurrence of both subcritical and supercritical Hopf bifurcations. Kwatny and Yu [7] give an example of a flutter instability in a three-machine classical network with lossy lines. Another example of a flutter instability is given by Rajagopalan *et al.* [11] in which a three-machine system is modeled with a two-axis representation and excitation is included.

When a flutter instability is observed in the linearized model, it is important to complete the analysis and to characterize the bifurcation completely. This is so because a loss in stability of the equilibrium point which is accompanied by the appearance of a small stable periodic motion (supercritical Hopf) may be of relatively minor concern whereas the existance of an unstable periodic motion near a stable equilibrium (subcritical Hopf) could portend catastrophic consequences following relatively minor disturbances. In this paper we present an approach to the analysis of Hopf bifurcations that may be conveniently applied to systems of reasonable scale. We show that the power system flutter instability of [7] corresponds to a supercritical Hopf bifurcation.

II. Model and Problem Definition

The dynamical equations of motion of the classical power system model may be written as [6]

$$\boldsymbol{M}\ddot{\delta} + \boldsymbol{D}\dot{\delta} + f_1(\delta,\phi,V,\mu) = 0 \tag{2.1a}$$

$$f_2(\delta,\phi,V,\mu) = 0 \tag{2.1b}$$

where $\boldsymbol{M}$ denotes the diagonal matrix of generator rotor inertias, $\boldsymbol{D}$ the damping matrix, δ the n-vector of generator internal bus angles, ϕ the $m+l$-vector of load bus angles, V the l-vector of PQ load bus voltage magnitudes, and μ a k-vector of network and load parameters. The functions f_1: $R^{n+m+2l+k} \to R^n$ and f_2: $R^{n+m+2l+k} \to R^{m+2l}$ are the usual load flow relations.

Let $(\delta^*,\phi^*,V^*,\mu^*)$ be an equilibrium point of (2.1). Suppose that the equilibrium point is *strictly causal* in the sense that there exist unique functions $\phi(\delta,\mu)$, $E(\delta,\mu)$ satisfying

Manuscript received October 17, 1989. This work was supported in part by the National Science Foundation under Grant ECS-871914. This paper was recommended by Associate Editor T. R. Viswanathan.

H. G. Kwatny is with the Department of Mechanical Engineering and Mechanics, Drexel University, Philadelphia, PA 19104.
G. E. Piper is with the Astro Space Division of General Electric, Princeton, NJ.

IEEE Log Number 9037944.

$f_2(\delta,\phi(\delta,\mu),V(\delta,\mu),\mu)=0$ in a neighborhood of $(\delta^*,\phi^*,V^*,\mu^*)$ with $\phi(\delta^*,\mu^*)=\phi^*$ and $V(\delta^*,\mu^*)=V^*$. Under these circumstances, (2.1) is locally equivalent to the system

$$M\ddot{\delta}+D\dot{\delta}+g(\delta,\mu)=0 \tag{2.2}$$

where $g(\delta,\mu)=f_1(\delta,\phi(\delta,\mu),V(\delta,\mu),\mu)$. Moreover, the linearized dynamics of (2.1) reduce to the form

$$M\ddot{x}+D\dot{x}+Kx=0 \tag{2.3}$$

where

$$K=\left\{D_\delta f_1-\begin{bmatrix}D_\phi f_1\\ D_E f_1\end{bmatrix}\begin{bmatrix}D_\phi f_2\\ D_E f_2\end{bmatrix}^{-1}D_\delta f_2\right\} \tag{2.4}$$

and $x=\delta-\delta^*$. In general, M is positive definite and D is positive semi-definite. The matrix K, however, is not typically symmetric. K depends on the parameter μ, both explicitly through the Jacobian matrices in (2.4) and implicitly through the variation of the equilibrium point with μ. Note also, that in the event that only constant admittance loads are present, then (2.2) is the global model with $g(\delta,\mu):=f_1(\delta,\mu)$. To simplify the following discussion we focus on this case.

In the absence of damping, the linearized power system model has the form

$$M\ddot{x}+Kx=0. \tag{2.5}$$

For a stable equilibrium of (2.5), all eigenvalues are on the imaginary axis. Kwatny and Yu [7] show that under load parameter variations, loss of stability occurs when a pair of imaginary eigenvalues meet and move off the imaginary axis. When the meeting takes place at $j\omega\neq 0$, the loss of stability of the equilibrium is typically accompanied by the presence of a limit cycle. Such bifurcation points usually correspond to either subcritical or supercritical Hopf bifurcations. This is the situation of interest. Thus we wish to analyze a transition of the eigenvalue pattern through the sequence: $(\pm j\omega_1,\pm j\omega_2)\rightarrow(\pm j\omega)^2\rightarrow(\pm\sigma\pm j\omega)$. The classical Hopf bifurcation theorem asserts that if a simple pair of conjugate eigenvalues cross the imaginary axis transversally at μ_0 $(D_\mu Re[\lambda(\mu_0)]\neq 0)$ then a periodic orbit exists for parameter values near μ_0.

The transition of the eigenvalue pattern for (2.5) does not satisfy the transversality condition of the Hopf bifurcation theorem. In fact, $D_\mu Re[\lambda(\mu)]$ does not exist at $\mu=\mu_0$. However, by strategically introducing small damping to the conservative power system mode the transversality condition can be induced. Damping in power systems arises in small amounts from many different sources and there is no universally accepted model of dissipation. For analytical convenience we will introduce uniform damping so that the normal modes of the conservative system are preserved.

$$D=\lambda M, \qquad \lambda \text{ is a positive scalar.} \tag{2.6}$$

The eigenvalue behavior as a function of μ is transformed by the introduction of uniform damping so that the transversality condition is satisfied, which allows us to apply the Hopf bifurcation theorem.

III. Frequency-Domain Analysis

To being our analysis, we rewrite (2.2) in first order form

$$\dot{x}=Ax+Bg(Cx,\mu) \tag{3.1}$$

where

$$x=\begin{bmatrix}\delta\\ \dot{\delta}\end{bmatrix}, \quad A=\begin{bmatrix}0 & I\\ 0 & -M^{-1}D\end{bmatrix},$$
$$B=\begin{bmatrix}0\\ -M^{-1}\end{bmatrix}, \quad C=[I \quad 0]. \tag{3.2}$$

Equations (3.1) can be formulated into infinitely many equivalent feedback representations by introducing an arbitrary $l\times m$ matrix R as follows:

$$\dot{x}=Ax+BRy+B[g(y,\mu)-Ry], \qquad y=Cx. \tag{3.3}$$

Taking the Laplace transform of both sides of (3.3) and solving for $\mathscr{L}(x)$ as a function of the Laplace variable s, then writing $e=-Cx$, we obtain

$$\mathscr{L}(e)=-G(s,\mu)\mathscr{L}(u) \tag{3.4a}$$

where

$$G(s,\mu)=C[sI-(A+BRC]^{-1}B \tag{3.4b}$$
$$u=f(e,\mu):=g(-e,\mu)-Ry. \tag{3.4c}$$

Equations (3.4) define a continuum of equivalent nonlinear multiple-loop feedback representations that have been separated into a dynamical linear part with a transfer matrix G and a memoryless nonlinear part f.

An equilibrium point of (3.4), e^*, satisfies the relation

$$G(0,\mu)f(e^*,\mu)=-e^*. \tag{3.5}$$

Stability of the equilibrium can be determined by linearizing (3.4c) at e^* and applying the multivariable Nyquist criterion [8]. The linearized system has open loop transfer function $G(s,\mu)J(\mu)$, where $J(\mu):=D_e f(e^*,\mu)$. Let $\lambda_i(s)$, $i,\cdots,n$, denote the characteristic functions associated with the open loop transfer matrix. If the open loop system has no uncontrollable and or unobservable modes with characteristic frequencies in the right-half plane then the closed loop system is stable if and only if the number of anticlockwise encirclements of the point $-1+j0$ by the set of characteristic loci of $G(s,\mu)J(\mu)$ is equal to the number of right-half plane poles of $G(s,\mu)J(\mu)$.

We assume that there is a critical value of μ, denoted μ_0, such that the linearized system has precisely one pair of simple imaginary eigenvalues $\pm j\omega_0$. This is equivalent to the open-loop matrix $G(j\omega_0,\mu_0)J(\mu_0)$ having precisely one eigenvalue at $-1+j0$. According to the Hopf bifurcation theorem, we expect (3.4) to exhibit an isolated periodic motion for μ sufficiently close to μ_0. In the frequency-domain Hopf bifurcation analysis, the periodic motion is approximated by a harmonic balance solution.

$$e(t)=e_0+\sum_{k=-\infty}^{\infty}E^k e^{jk\omega t} \tag{3.6a}$$

$$u(t)=u_0+\sum_{k=-\infty}^{\infty}U^k e^{jk\omega t}. \tag{3.6b}$$

Since $e(t),u(t)$ are real valued functions, the Fourier coefficients satisfy the relations

$$E^{-k}=\bar{E}^k, \qquad U^{-k}=\bar{U}^k.$$

The coefficients are related across the linear part of the system by

$$E^k=-G(j\omega,\mu)U^k. \tag{3.7}$$

Since the amplitude of the limit cycle is assumed to be small for μ near μ_0 (so that $e(t)$ remains near e_0), it is reasonable to

characterize the nonlinearity by its Taylor series

$$f(e,\mu)=f(e_0,\mu)+\sum_{k=1}^{\infty}\frac{1}{k!}\left(D_e^k f\right)\cdot\left[(e-e_0)\otimes\right]^{k-1}(e-e_0). \tag{3.8}$$

Substituting the Fourier expansions of e and u, retaining only second-order harmonics and equating coefficients yields

$$U^1=JE^1+P(\omega,E^1)+O\left(|E^1|^4\right) \tag{3.9}$$

where

$$P(\omega,E^1)=-\frac{1}{4}\left(D_e^2 f\right)\cdot\left[H(0)\left(D_e^2 f\right)\cdot E^1\cdot\bar{E}^1\otimes E^1+\bar{E}^1\otimes H(2j\omega)\cdot\left(D_e^2 f\right)\cdot E^1\cdot E^1\right]+\frac{1}{8}\left(D_e^3 f\right)\cdot E^1\otimes E^1\otimes\bar{E}^1 \tag{3.10}$$

$$H(s)=(G(s)J+I)^{-1}G(s).$$

Thus E^1 is determined up to terms of fourth order by the loop equation

$$[G(j\omega,\mu)J+I]E^1=-G(j\omega,\mu)P(\omega,E^1). \tag{3.11}$$

Before stating the frequency-domain Hopf bifurcation theorem let $\lambda(j\omega)$ denote the characteristic function of $G(j\omega,\mu)J(\mu)$, which intersects the real axis nearest to the point $-1+j0$, the intersection occurring at $\omega=\omega_r$. Also, let w,v denote, respectively, the left and right eigenvectors of $G(j\omega_r,\mu)J(\mu)$. Now, define the complex valued function

$$\zeta(\omega_r)=\frac{-w^t G(j\omega_r,\mu)P(\omega_r,v)}{w^t v}. \tag{3.12}$$

From [9], we have the following result.

Theorem 3.1: Suppose g in (3.1) is C^4, $\zeta(\omega_r)$ given by (3.12) is nonzero, and the half line $-1+\theta^2\zeta(\omega_r)$, θ real and ≥ 0, intersects the curve $\lambda(j\omega)$ transversally at a point P' with $\lambda(j\omega')=-1+\theta'^2\zeta(\omega_r)$. If there are no other intersections of any of the characteristic loci of $G(j\omega,\mu)J(\mu)$ and the closed line segment connecting $-1+j0$ to P', then there exists $\theta_0\geq\theta_1>0$ and $\omega_0\geq\omega_1>0$ such that

a) if $\theta'<\theta_0$ and $|\omega'-\omega_r|<\omega_0$, the system (3.1) has a periodic solution $e(t)$ of frequency $\omega=\omega'+O(\theta'^4)$ and such that

$$e(t)=e_0+\sum_{k=-2}^{2}E^k e^{jk\omega t}+O(\theta^3)$$

and b) this periodic orbit is unique in a ball centered at x_0 and of radius $O(1)$. If $\theta'<\theta_1$ and $|\omega'-\omega_r|<\omega_1$, the periodic orbit is the unique attractor in a ball centered at x_0 and of radius $O(1)$ if the following encirclement condition holds: the total number of anticlockwise encirclements of the point $P'+\delta\zeta(\omega_r)$ by the characteristic loci λ_k is equal to the number of poles of $\lambda_k(s)$ with positive real part. $\delta>0$ is chosen sufficiently small that no new intersections between the locus and the half line are introduced.

Proof of this theorem along with an enlightening discussion may be found in [9]. It is shown that E^1 is $O(\theta)$ and in fact the parameter θ may be thought of as the amplitude of the limit cycle. The importance of this result is that it retains much of the convenience of Nyquist and describing function analysis for systems of large dimension while at the same time it is based on a rigorous theoretical framework. Moreover it is applicable to systems with multiple nonlinearities.

IV. An Example

To illustrate how the frequency-domain Hopf bifurcation theorem can be adapted to electric power networks, we will apply it to the three-machine four-bus example presented in [7]. Bus 1 was taken as the swing bus and the reduced swing equations were written as

$$\ddot{\theta}_1+2D_{12}\sin(\theta_1)+D_{23}\sin(\theta_1-\theta_2)+D_{13}\sin(\theta_2)+C_{23}\cos(\theta_1-\theta_2)-C_{13}\cos(\theta_2)=\Delta P_1 \tag{4.1a}$$

$$\ddot{\theta}_2+2D_{13}\sin(\theta_2)+D_{23}\sin(\theta_2-\theta_1)+D_{12}\sin(\theta_1)+C_{23}\cos(\theta_2-\theta_1)-C_{12}\cos(\theta_1)=\Delta P_2 \tag{4.1b}$$

where $\theta_1=\delta_2-\delta_1$, $\theta_2=\delta_3-\delta_1$, $\Delta P_1=P_2-P_1$ and $\Delta P_2=P_3-P_1$. Note that δ_i, P_i denote, respectively, the ith machine angle and net power.

Kwatny and Yu [7] identified sets of parameter values that correspond to bifurcation points of the conservative system. Case 4 in that paper is generic in one-parameter families and is indicative of a Hopf bifurcation. This is the case of interest in the present analysis. The parameter values corresponding to this bifurcation point are shown in the following.

C_{12}	C_{13}	C_{23}	D_{12}	D_{13}	D_{23}	ΔP	ΔP_2	P_1	θ_1	θ_2
0	0	2	1	.5774	.5774	4.042	2.887	−1.155	1.047	0.5236

Adding uniform damping, (4.1) can be written in first-order form of (3.1) where

$$x=\begin{bmatrix}\theta\\ \dot{\theta}\end{bmatrix},\quad A=\begin{bmatrix}0 & I\\ 0 & -\lambda I\end{bmatrix},\quad B=\begin{bmatrix}0\\ I\end{bmatrix},\quad C=[I\quad 0]$$

$$g(Cx,\mu)=\begin{bmatrix}P_2-\mu-2D_{12}\sin(\theta_1)-D_{23}\sin(\theta_1-\theta_2)-D_{13}\sin(\theta_2)-C_{23}\cos(\theta_1-\theta_2)+C_{13}\cos(\theta_2)\\ P_3-\mu-2D_{13}\sin(\theta_2)-D_{23}\sin(\theta_2-\theta_1)-D_{12}\sin(\theta_1)-C_{23}\cos(\theta_2-\theta_1)+C_{12}\cos(\theta_1)\end{bmatrix},\qquad \mu=P_1.$$

Our next task is to transform (4.1) into an equivalent feedback system as in (3.4). One simple choice is to let the matrix $R=0$ in (3.3). However, a simple calculation shows that at $s=0$, $G(s)$ is undefined. Therefore, we choose $R=I$ to avoid singularities on the Nyquist contour, which gives us

$$G(s)=\begin{bmatrix}\dfrac{1}{s^2+\gamma s-1} & 0\\ 0 & \dfrac{1}{s^2+\gamma s-1}\end{bmatrix} \tag{4.2a}$$

$$f(e,\mu)=g(-e,\mu)+e. \tag{4.2b}$$

The Jacobian, $J=D_e f$, is

$$D_e f=\begin{bmatrix}\alpha+z & \beta+y\\ \beta-y & \alpha-z\end{bmatrix} \tag{4.3}$$

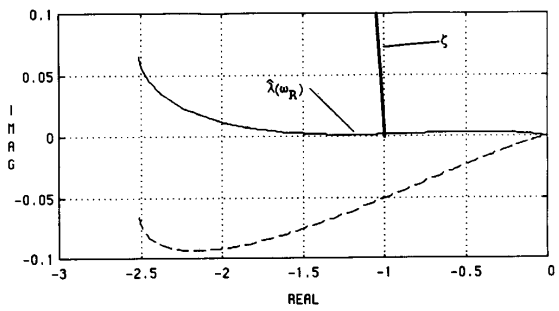

Fig. 1. The postbifurcation principal loci branches corresponding to $P_1 = -1.144$, $e^* = (-1.040, -0.5168)$, $\omega_r = 1.05$ r/s.

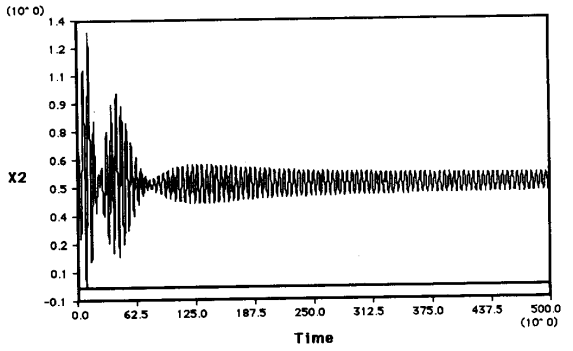

Fig. 2. Asymptotic attraction to the limit cycle of a postbifurcation trajectory initially far from the equilibrium point; $P_1 = -1.144$.

where

$$\alpha = D_{12}\cos(e_1) + D_{13}\cos(e_2) + D_{23}\cos(e_1 - e_2) + 1 \quad (4.4a)$$

$$z = D_{12}\cos(e_1) - D_{13}\cos(e_2)] + C_{23}\sin(e_2 - e_1) \quad (4.4b)$$

$$\beta = -D_{23}\cos(e_1 - e_2) + \{D_{12}\cos(e_1) + D_{13}\cos(e_2)\}/2 + \{C_{12}\sin(e_1) + C_{13}\sin(e_2)\}/2 \quad (4.4c)$$

$$y = \{D_{13}\cos(e_2) - D_{12}\cos(e_1)\}/2 + C_{23}\sin(e_1 - e_2) + \{-C_{12}\sin(e_1) + C_{13}\sin(e_2)\}/2 \quad (4.4d)$$

thus

$$G(s)J = \frac{1}{s^2 + \gamma s - 1}\begin{bmatrix} \alpha + z & \beta + y \\ \beta - y & \alpha - z \end{bmatrix}. \quad (4.5)$$

The characteristic functions of $G(j\omega)J$ are

$$\lambda(j\omega) = -\left\{\alpha \pm \sqrt{z + \beta - y}\right\}\frac{(\omega^2 + 1) + j\omega\gamma}{\omega^4 + (2+\gamma)\omega^2 + 1}. \quad (4.6)$$

It can be seen that the pole polynomial, defined in terms of the Smith–McMillam form [5], of the open loop transfer function matrix $G(s)J$ is

$$p(s) = (s^2 + \gamma s - 1)^2 \quad (4.7)$$

implying that $G(s)J$ has two positive real poles and two negative real poles. The generalized Nyquist stability criterion states that the number of encirclements of the point $(-1 + j0)$ by the characteristic loci must equal to the number of poles in the right-half plane for the closed loop system to be stable. Since $G(s)J$ has two positive real poles the characteristic loci must encircle the point $(-1 + j0)$ twice to indicate that the system is stable.

Setting $\gamma = 0.05$ and using the parameter values listed, we have performed the necessary computations as the bifurcation parameter P_1 is varied through its critical value. Note that the critical value of P_1 is shifted from -1.155 to approximately -1.146 with introduction of the uniform damping $\gamma = 0.05$. For $P_1 < -1.146$, the characteristic loci encircle $(-1 + j0)$ twice indicating a stable system. As P_1 approaches its critical value, a locus approaches $(-1 + j0)$. When P_1 passes through its critical value, the the locus passes through $(-1 + j0)$ and no longer encircles it, indicating an unstable system as shown in Fig. 1. This behavior of the characteristic loci corresponds to the crossing of imaginary axis by two system eigenvalues of the linear system.

The correction vector, ζ, was calculated and is shown in Fig. 2. We see that one of the loci intersects with ζ, which indicates that a limit cycle does exists. Using the perturbation argument from above (part b of Theorem 3.1) implies that the limit cycle is stable. The frequency of the limit cycle is approximately the same as the frequency associated to the bifurcation point.

To verify our analysis, (4.2) were integrated with a Runge–Kutta program. The system converges to the equilibrium for prebifurcation conditions. Fig. 2 corresponds to the conditions in Fig 1. The system converges to a steady state oscillation with frequency = 1.2 rad/s which is close to the predicted value.

V. Conclusions

In this paper we have shown how the frequency-domain version of the Hopf bifurcation theorem can be applied to the analysis of flutter instability in electric power networks. Such instabilities have appeared in the literature with increasing frequency in recent years and are evidently induced by heavy loading of the transmission system. The frequency-domain analysis not only establishes the existence of a limit cycle but provides a convenient test for stability. We emphasize the practical importance of establishing the type of Hopf bifurcation, i.e., subcritical or supercritical. Systems that operate near a subcritical Hopf bifurcation point are clearly vulnerable to disturbances.

One of our objectives has been to complete the analysis pertaining to the flutter instability identified in the three-machine network used as an example in [7]. It has been shown that the instability encountered therein is indeed a Hopi bifurcation and that it is supercritical. The results of the analysis have been verified by computer simulation.

Finally, we note that the frequency-domain analysis is extremely simple to carry out on our small example and shows feasibility for application to systems of larger scale and with more complex models.

References

[1] E. Abed and P. P. Varaiya, "Nonlinear oscillations in power systems," *Int. J. Elec. Power and Energy Syst.*, vol. 6, pp. 37–43, 1984.
[2] J. C. Alexander, "Oscillatory solutions of a model system of nonlinear swing equations," *Int. J. Elec. Power and Energy Syst.*, vol. 8, pp. 130–136, 1986.
[3] A. Araposthatis, S. Sastry, and P. Varaiya, "Global analysis of swing dynamics," *IEEE Trans. Circuits Syst.*, vol. CAS-29, pp. 673–679, Oct. 1982.
[4] S-N. Chow and J. K. Hale, *Methods of Bifurcation Theory*. New York: Springer-Verlag, 1982.
[5] T. Kailath, *Linear Systems*. Englewood Cliffs, NJ: Prentice-Hall, 1980.
[6] H. G. Kwatny, A. K. Pasrija, and L. Y. Bahar, "Static bifurcations in electric power networks: Loss of steady-state stability and voltage collapse," *IEEE Trans. Circuits Syst.*, vol. CAS-33, pp. 981–991, Oct. 1986.

[7] H. G. Kwatny and X-M. Yu, "Energy analysis of load-induced flutter instability in classical models of electric power networks," *IEEE Trans. Circuits Syst.*, vol. 36, pp. 1544–1557, Dec. 1989.
[8] A. G. J. MacFarlane and Postlethwaite, "The generalized Nyquist stability criterion and multivariable root loci," *Int. J. Contr.*, vol. 25, pp. 81–127, 1977.
[9] A. Mees and L. Chua, "The Hopf bifurcation theorem and its applications to nonlinear oscillations in circuits and systems," *IEEE Trans. Circuits Syst.*, vol. CAS-26, pp. 235–254, Apr. 1979.
[10] J. E. van Ness, F. M. Brash, Jr., G. L. Landgren, and S. I. Neumann, "Analytic investigation of dynamic instability occurring at powerton station," *IEEE Trans. Power App. Syst.*, vol. PAS-99, pp. 1386–1395, July/Aug. 1980.
[11] C. Rajagopalan, P. W. Sauer, and M. A. Pai, "An integrated approach to dynamic and static voltage stability," in *Proc. American Control Conf.*, pp. 1231–1236, June 1989.
[12] V. A. Venikov, V. A. Stroev, V. I. Idelchick, and V. I. Tarasov, "Estimation of electric power system steady-state stability in load flow calculations," *IEEE Trans. Power App. Syst.*, vol. PAS-94, pp. 1034–1038, May/June 1975.

On Computing 2-D Systolic Algorithm for Discrete Cosine Transform

MOON HO LEE

Abstract—**In this paper, we propose an algorithm on a two-dimensional systolic array for discrete cosine transform (DCT). It is based on the inverse DFT version of the Goertzel algorithm via Horner's rule. This array requires N cells and multipliers, takes $\sqrt{N+2}$ clock cycles to produce a complete N-point DCT, and is able to process a continuous stream of data sequences.**

I. Introduction

In recent years, there has been a growing interest regarding the applications of the discrete transforms to digital signal processing [1], [2]. The DCT is usefully accepted as the best suboptimal transformation for picture coding [3]. To minimize the computation time, researchers have recently been trying to integrate the complete transformation process on to a single VLSI chip. Jutand *et al.* reported the design of a processor for two-dimensional (2-D) DCT, which was the row–column decomposition [4].

Because of the neat optimal property of the DCT, it is widely used in the processing of 2-D signals. In particular, it has been found to be useful in the transform domain coding of TV images in real time. Many processors have been designed to meet the real time throughput requirements of these applications. Fast DCT algorithms follow the matrix decomposition itself and the other discrete transform.

Although the various algorithms for signal processing are implemented in the systolic architecture, fast DCT algorithms, which are proposed by Chen and Lee [5], [6], are difficult to implement in the systolic architecture because they lack the regularity and local connectivity in the signal flow graph. In contrast, to overcome these problems, a fast DCT algorithm for systolic array is derived from a $4N$-point Winograd–Fourier transform [7].

In this paper, we divide the DCT into the inverse DFT(IDFT) and the multiplication part in order to realize a 2-D systolic array for DCT. The transformation into 2-D index space and the Goertzel algorithm via Horner's rule allowed the DCT to be mapped onto 2-D systolic array, which is a modular processor array with local communication. The computational time of this 2-D systolic array is faster than that of the 1-D systolic array [8]. This array is flexible and can be made compatible with other orthogonal transforms by changing the array coefficients [9].

Manuscript received November 3, 1989. This paper was recommended by Associate Editor T. R. Viswanathan.
M. H. Lee is with the Department of Information and Telecommunications Engineering, Chonbuk National University, Chonju 560-756, Korea.
IEEE Log Number 9034714.

II. 2-D Systolic Array for DCT

The N-point DFT is defined as

$$X(k)=\sum_{n=0}^{N-1} x(n)W_N^{nk} \tag{1}$$

for $k=0,1,\cdots,N-1$, where $W_N=\exp(-j2\pi/N)$.

If $N=p\cdot q$, in order to process 1-D DFT in the 2-D systolic array, we define the following mapping index between the input and output data.

$$n=ij$$
$$k=rt \tag{2}$$

where $ij=qi+j$, $rt=pr+t$, and $0\leqslant i,t\leqslant p-1$, $0\leqslant j,r\leqslant q-1$. Therefore, the N-point DFT of a sequence $x_0,x_1,\cdots,x_{pq-1}$, is defined as follows [10]:

$$X_{rt}=\sum_{i=0}^{p-1}\sum_{j=0}^{q-1} X_{ij}W_N^{(pr+t)(qi+j)} \tag{3}$$

for $r=0,1,\cdots,q-1$ and $t=0,1,\cdots,p-1$, where r,t denotes the column and row index of the output data from the PE's, and i,j represents the row and column index of the input data, fed into the PE's.

The DCT of a data sequence $f(n)$, $n=0,1,\cdots,N-1$ is defined by [3]

$$F(k)=C(k)\sum_{n=0}^{N-1} f(n)\cos[(2n+1)k\pi/2N] \tag{4}$$

for $k=0,1,\cdots,N-1$, where $C(k)=\{1/\sqrt{2}$, for $n=0$, and 1, for $n=1,2,\cdots,N-1$. Assuming N is even, define a new N-point sequence $x(n)$ by [11]

$$x(n)=f(2n)$$
$$x(N-1-n)=f(2n+1),\qquad n=0,1,\cdots,N/2-1. \tag{5}$$

With this substitution (4), can be rewritten as

$$F(k)=C(k)\left\{\sum_{n=0}^{N/2-1} x(n)\cos[(4n+1)k\pi/2N] + \sum_{n=0}^{N/2-1} x(N-1-n)\cos[(4n+3)k\pi/2N]\right\}. \tag{6}$$

Letting $n'=N-1-n$ in the second sum, simplifying and recombining the two sums yields

$$F(k)=C(k)\sum_{n=0}^{N-1} x(n)\cos[(4n+1)k\pi/2N]. \tag{7}$$

Thus the DCT $F(k)$ can be evaluated as

$$F(k)=C(k)\,\mathrm{Re}\{\exp[jk\pi/2N]\cdot Z(k)\} \tag{8}$$

0098-4094/90/1000-1321$01.00 ©1990 IEEE